

An intense and broad Fe K $_{\alpha}$ line observed in the X-ray luminous quasar Q 0056-363 with XMM-Newton

D. Porquet¹ and J.N. Reeves^{2,3}

¹ Max-Planck-Institut für extraterrestrische Physik, Postfach 1312, D-85741, Garching, Germany

² Laboratory for High Energy Astrophysics, Code 662.0, NASA Goddard Space Flight Center, Greenbelt, MD 20771, USA

³ Universities Space Research Association

Received January 20, 2003 / Accepted June 16, 2003

Abstract. We present an *XMM-Newton* observation of the radio-quiet quasar Q0056-363 ($z=0.162$). This is the first time that this quasar is observed in the hard X-ray range (above 2 keV). We find that Q0056-363 is a powerful X-ray quasar, with a 0.3–12 keV unabsorbed luminosity of about 1.2×10^{45} erg s $^{-1}$ with the largest part ($\sim 67\%$) emitted below 2 keV. The spectrum reveals a large featureless soft X-ray excess below 2 keV and a strong broad Fe K $_{\alpha}$ line at 6.4 keV (in the quasar frame). The Fe K $_{\alpha}$ line is due to low to moderate ionization states of iron (i.e., $< \text{Fe XVII}$), with an equivalent width of about 250 eV and a velocity width of about 25,000 km s $^{-1}$. Q0056-363 is presently the most luminous AGN known to exhibit such a broad and intense Fe K $_{\alpha}$ line profile from near neutral iron. The line can be fitted with a relativistic profile from an accretion disc around either a Schwarzschild (non-rotating) or a Kerr (rotating) black hole. A combination of two thermal Comptonization components and a disc reflection model is favored to explain both the continuum over the energy range 0.3–12 keV and the Fe K $_{\alpha}$ line. A patchy corona covering a large part of the inner disc surface is needed in order to be compatible with the accretion rate inferred from the spectral energy distribution of Q0056-363, unless the mass of the black hole is much higher than about $5 \times 10^8 M_{\odot}$.

Key words. galaxies: active – X-rays: galaxies – accretion discs – quasars: individual: Q0056-363

1. Introduction

In Active Galactic Nuclei (AGN), from Seyfert galaxies to quasars, several X-ray features can help us to understand the central region of these powerful objects. The first one is the so-called soft excess seen below 2–3 keV (Arnaud et al. 1985; Turner & Pounds 1989). This spectral characteristic is thought to be the high energy part of the “big blue bump” (BBB) extending down to $1 \mu\text{m}$, which contains a large fraction of the bolometric luminosity. Recently Pounds & Reeves (2002), using *XMM-Newton* observations, showed that a soft X-ray excess is seen in all their sample (6 Seyfert galaxies) with an amplitude and a breadth increasing with luminosity. Current interpretations of the soft excess range from intrinsic thermal emission from the accretion disc, to reprocessing of harder radiation absorbed in the thin disk (Pounds & Reeves 2002). Another important component is emission and/or absorption, mainly in the soft X-ray range, due to the Warm Absorber medium supposed to be located between

the Broad Line Region and the Narrow Line Region (e.g., Reynolds & Fabian 1995; Porquet et al. 1999). However these absorption and/or emission features seem to be only seen in low-luminosity AGN, such as Seyfert galaxies. The Fe K $_{\alpha}$ line complex observed in the 6–7 keV range is also an important spectral tool. Indeed the study of this fluorescent line complex allows us to probe dense matter from the inner disc to the molecular torus as found recently in several AGN (e.g. Mrk 205, Reeves et al. 2001; Mrk 509, Pounds et al. 2001).

In this paper we present an *XMM-Newton* observation of Q0056-363, a radio-quiet quasar ($z = 0.162$, Hewitt & Burbidge 1989; $\alpha_{J2000}=00^{\text{h}}58^{\text{m}}37.38^{\text{s}}$, $\delta_{J2000}=-36^{\circ}06'04.8''$, 2MASS, Cutri et al. 2003) detected for the first time in the ESO B Southern Sky Survey (Monk et al. 1986). It has strong, broad permitted optical emission lines (e.g., $\text{FWHM}(\text{H}\beta)=4700 \pm 160$ km s $^{-1}$, Grupe et al. 1999), which led to it being described as a Broad-Line Seyfert 1 AGN. Until now, this quasar was only observed in the X-ray domain by *ROSAT*, i.e. below 2.4 keV (RASS: Thomas et al. 1998, HRI: Grupe et al.

Send offprint requests to: D. Porquet

Correspondence to: dporquet@mpe.mpg.de

Table 1. Summary of the data used to build the spectral energy distribution of Q0056-363. C03: Cutri et al. (2003). M03: Monet et al. (2003). UVW2 is the OM filter used during the present *XMM-Newton* observation. G99: Grupe et al. (1999). INES: Merged Log of *IUE* Observations (NASA-ESA, 1999).

Filter wavelength or energy band	magnitude or flux	Observation date	reference
K _s	12.301±0.032 mag	07/1999	C03
H	13.390±0.044 mag	07/1999	C03
J	14.228±0.037 mag	07/1999	C03
I	14.69 mag	02/1987	M03
[6600-7820Å] (Red)	(spectrum)	10/1993	G99
[4640-5950Å] (Blue)	(spectrum)	10/1993	G99
OM (UWV2)	2.11±0.04 erg cm ⁻² s ⁻¹ Å ⁻¹	07/2000	this work
IUE (UV: [1151-1979Å])	(spectrum)	10/1995	INES
XMM (X-rays: 0.3-10 keV)	(spectrum)	07/2000	this work

2001). We present here the first observation of this object in the hard X-ray range up to 12 keV.

Note that all fit parameters are given in the quasar’s rest frame, with values of $H_0=50 \text{ km s}^{-1} \text{ Mpc}^{-1}$, and $q_0=0$ assumed throughout. The errors quoted correspond to 90% confidence ranges for one interesting parameter ($\Delta\chi^2=2.71$). Abundances are those of Anders & Grevesse (1989). In the following, we use the updated cross-sections for X-ray absorption by the interstellar medium from Wilms et al. (2000).

2. XMM-Newton observation

We present an archived *XMM-Newton* observation of Q0056-363 on July 5, 2000 (ID 0102040701; orbit 145; exposure time ~ 20 ks). The EPIC MOS cameras (Turner et al. 2001) operated in the Small Window mode, while the EPIC PN camera (Strueder et al. 2001) was operated in the standard Full Frame mode. For operational reasons, the MOS observations are divided into two separate exposures of ~ 5 ks, one with the thin filter and the other one with the thick filter. Since the MOS data give considerably lower net counts compared to the PN data (thin filter), we proceed to use only the PN for the present analysis. The data are re-processed and cleaned (net time exposure ~ 14.8 ks) using the *XMM-Newton* SAS VERSION 5.3.3 (Science Analysis Software) package. Since pile-up effect is negligible according to the EPATPLOT SAS task, X-ray events corresponding to patterns 0–4 events (single and double pixels) are selected for the PN. A low-energy cutoff is set to 300 eV. The source spectrum and the light curve are extracted using a circular region of diameter 40'' (to avoid the edge of the chip) centered on the source position. Q0056-363 is by far the brightest X-ray source in this 30' EPIC field-of-view. Background spectra are taken from an annular radius center on Q0056-363, between 4' and 8' (excluding X-ray point sources, and the columns passing through the source to avoid out-of-time events). The XSPEC v11.2 software package is used for spectral anal-

ysis of the background-subtracted spectrum using the response matrices and ancillary files derived from the SAS tasks RMFGEN and ARFGEN. The PN spectrum is binned to give a minimum of 20 counts per bin.

Data from the Reflection Grating Spectrograph (RGS; den Herder et al. 2001) are also re-processed using the SAS RGSPROC script, giving effective exposure time of 19.5 ks and 18.9 ks. The signal to noise ratio is not sufficient for reliable RGS data analysis.

The OM took a sequence of 4 exposures (1000s each) through the UVW2 filter. We calculate for all exposures the UV fluxes; these are, 2.10 ± 0.04 , 2.14 ± 0.04 , 2.11 ± 0.04 , and 2.08 ± 0.04 respectively, expressed in units of $10^{-14} \text{ erg cm}^{-2} \text{ s}^{-1} \text{ Å}^{-1}$. All values are compatible within the error bars indicating no appreciable UV variability.

3. Spectral energy distribution of Q0056-363: bolometric luminosity, and accretion rate

We use the K_s, H and J magnitudes from the 2MASS point source catalog released in March 2003 (Cutri et al. 2003, <http://www.ipac.caltech.edu/2mass/>), and the I magnitude from the USNO-B Catalog (Monet et al. 2003). To convert these magnitude in flux we use the Johnson UBVR photometric system (Campins et al. 1985). We use the optical spectra from Grupe et al. (1999, ESO/MPI 2.2m telescope) in the Red and Blue range. The UV spectrum is from an *IUE* observation (NASA-ESA, 1999, <ftp://archive.stsci.edu/pub/iue/data/>). The X-ray part is the unabsorbed *XMM-Newton* PN spectrum (this work). Up to now Q0056-363 is not yet observed above 12 keV. Table 1 reports the observation dates and references. We take into account the Galactic extinction using $E(B-V)=0.014$ mag (Schlegel et al. 1998), using the extinction formulae from Seaton (1979) for the UV, from O’Donnell (1994) for the optical and from Ryter (1996) for the IR. The spectral energy distribution for Q0056-363 is reported in Fig. 1.

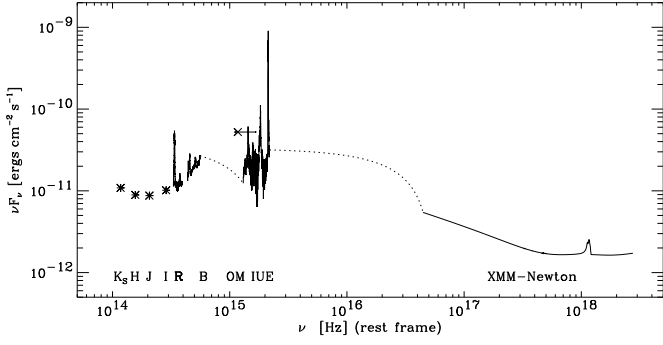


Fig. 1. Spectral energy distribution of Q0056-363. The references of magnitudes, fluxes, and spectra are reported in Table 1.

Summing the integrated fluxes, from K_s and B bands, inside the *IUE* and the *XMM-Newton* domains, we estimate a luminosity of $6 \times 10^{45} \text{ ergs}^{-1}$. We find that the luminosities in the *IUE* and *XMM-Newton* domains are about $2.0 \times 10^{45} \text{ ergs}^{-1}$ and $1.2 \times 10^{45} \text{ ergs}^{-1}$, respectively. If we take into account the linearly interpolated fluxes between the *B* and the *IUE* domains, and between the *IUE* and *XMM-Newton* spectra (see Fig. 1), we find a bolometric luminosity of about $4.4 \times 10^{46} \text{ ergs}^{-1}$. We notice that the largest part of the Eddington luminosity (i.e. $\sim 80\%$) is emitted between the *IUE* and *XMM-Newton* domain, where there is no data due to absorption by neutral hydrogen located in our Galaxy, between about 100 \AA (120 eV) and 912 \AA (13.6 eV).

According to the relation between the black hole (BH) mass and the width and strength of the H_β line measured in Grupe et al. (1999), we infer a BH mass in Q0056-363 of about $4.5 \times 10^8 M_\odot$ or of about $6.1 \times 10^8 M_\odot$ using the formulae from McLure & Dunlop (2002) and McLure & Jarvis (2002) respectively. The Eddington luminosity ($L_{\text{Edd}} = 1.26 \times 10^{38} M_{\text{BH}}/M_\odot$) is then $5.7 \times 10^{46} \text{ ergs}^{-1}$ ($7.7 \times 10^{46} \text{ ergs}^{-1}$) for $M_{\text{BH}} = 4.5 \times 10^8 M_\odot$ ($M_{\text{BH}} = 6.1 \times 10^8 M_\odot$). Then the accretion rate values, as a fraction of the Eddington rate (i.e. $\dot{m} = \dot{M}/\dot{M}_{\text{Edd}} = L_{\text{bol}}/L_{\text{Edd}}$) are 0.77 and 0.57 for $M_{\text{BH}} = 4.5 \times 10^8 M_\odot$ and $M_{\text{BH}} = 6.1 \times 10^8 M_\odot$, respectively.

4. Spectral analysis

We find an average count rate in the 0.3–12 keV energy range for the PN data of $2.84 \pm 0.01 \text{ cts s}^{-1}$. The light curve does not show any evidence of variability, a fit to a constant count rate is acceptable (yielding a χ^2 of 148 for 163 degrees of freedom). As there is no significant variability detected during this observation, we sum the data over the whole observation. First, a single absorbed power-law model is fitted to the overall 0.3–12 keV PN spectrum, but we find a poor fit ($\chi^2_{\text{red}} = 1.43$ for 527 d.o.f. with $\Gamma = 2.43^{+0.02}_{-0.01}$). We find no additional absorption, located at the quasar redshift, compared to the Galactic column

density (i.e., $1.88 \times 10^{20} \text{ cm}^{-2}$). Therefore in all subsequent fits, the column density is fixed to the Galactic value.

To characterize the hard X-ray continuum, we fit an absorbed power-law model over the 2.5–5 keV energy range where the spectrum should be relatively unaffected by the presence of a broad soft excess, a Warm Absorber-Emitter medium, an FeK α emission line, and of a contribution above 8 keV from a high energy Compton reflection hump. In this energy range, the data are well fitted by a single power-law model with $\Gamma = 2.03 \pm 0.18$ ($\chi^2/\text{d.o.f.} = 90.3/98$). Fig. 2 displays the spectrum extrapolated over the 0.3–12 keV broad band energy. A strong positive residual is clearly seen below 2 keV due to the presence of a soft X-ray excess. In addition, a strong deviation near 5.5 keV (6.4 keV in the quasar rest-frame) is seen, suggesting the presence of a FeK α line complex.

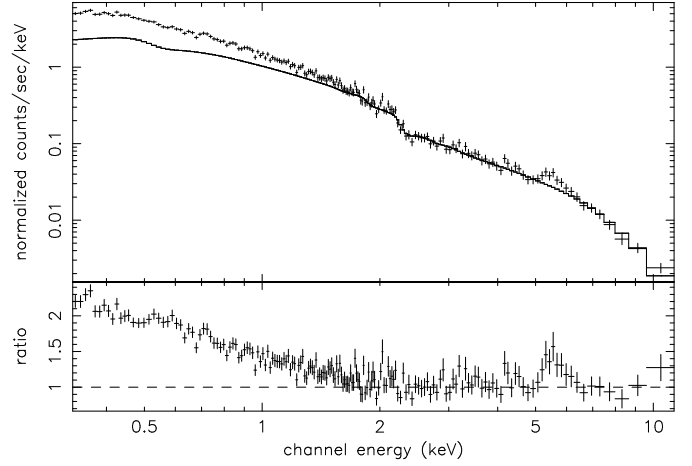


Fig. 2. The PN spectrum of Q0056-363 (in the observer frame). A power-law has been fitted to the 2.5–5 keV data and extrapolated to lower and higher energies. A broad, strong soft X-ray excess is clearly seen extending to ~ 2 keV, as well as a strong deviation near 5.5 keV, suggesting the presence of a FeK α line. For presentation, the data have been re-binned into groups of 3 bins, after group of a minimum of 20 counts per bin is used for the fit.

4.1. The soft excess below 2 keV

Next, we fit the 0.3–2 keV energy range with a single absorbed power-law, and find a reasonable fit with a photon index of $\Gamma = 2.53 \pm 0.02$ ($\chi^2/\text{d.o.f.} = 338.8/327$). This value is compatible with $\Gamma = 2.7 \pm 0.2$ (Grupe et al. 1999) and with the slope between 2500 \AA and 2 keV of $\Gamma = 2.62 \pm 1.51$ inferred from December 1990 observation (*ROSAT* All-Sky Survey, Grupe et al. 2001). The 0.3–5 keV energy range is well fitted by the combination of a blackbody and a power-law component. We find $kT_{\text{bb}} = 133 \pm 7 \text{ eV}$ and $\Gamma = 2.28 \pm 0.02$ ($\chi^2/\text{d.o.f.} = 505.7/474$). Since the soft-excess feature is both large and broad, we add two other blackbody components and a better fit is obtained: $kT_{\text{bb}1} = 30^{+3}_{-2} \text{ eV}$, $kT_{\text{bb}2} = 122 \pm 4 \text{ eV}$, $kT_{\text{bb}3} = 273 \pm 10 \text{ eV}$, and $\Gamma = 1.93^{+0.09}_{-0.02}$.

($\chi^2/\text{d.o.f.}=472.7/471$). The three blackbody components represent a large percentage (compared to the power-law component) of the total flux in the 0.3–2 keV energy range, of $51_{-3}^{+47}\%$. The high-energy power-law slope in the multi-component model is consistent with the $\Gamma=1.9$ index commonly seen in radio-quiet quasars (e.g. Reeves & Turner 2000). In order to obtain a more physical representation of the soft excess, we also test multi-temperature disc models, which may be expected if the soft X-ray excess originates via thermal emission from the inner accretion disc in Q0056-363. The DISKBB (non-relativistic) and DISKPN (relativistic) models within XSPEC are used, together with a power-law to model the hard X-ray emission above 2 keV. Equally good fits are obtained for both models. For the first model we find $kT_{\text{diskbb}}=161\pm 9$ eV and $\Gamma=2.21\pm 0.05$ ($\chi^2/\text{d.o.f.}=495.6/474$), and similar parameters are found for the second model with $kT_{\text{diskpn}}=153_{-8}^{+7}$ eV and $\Gamma=2.21_{-0.02}^{+0.05}$ ($\chi^2/\text{d.o.f.}=495.4/474$). The inner disc temperatures obtained through either of these models appear to be unusually high, for what one would expect from a standard steady state α thin accretion disc. Assuming a BH mass of about $4.5\text{--}6\times 10^8 M_{\odot}$, we expect a maximum temperature of only about 15 eV at $3R_{\text{S}}$ (e.g. Peterson 1997).

We find no evidence for significant intrinsic cold or warm absorption. Adding two absorption edges of O VII (0.7 keV) or O VIII (0.87 keV), we infer edge optical depth limits of $\tau < 0.1$. The lack of significant spectral absorption features implies that we are seeing the bare quasar continuum emission.

4.2. The FeK $_{\alpha}$ line near 6.4 keV

As shown in Fig.2, a very strong deviation is seen near 5.5 keV in the observer frame, i.e. about 6.4 keV in the quasar frame. In the overall 2.5–12 keV energy band, adding a Gaussian line to a single power-law model drops the χ^2 value by 17 with the addition of 3 degrees of freedom (Table 2), significant at $> 99.95\%$ according to the F-test. Adding an ionised emission line and an absorption edge do not improve the fit ($\Delta\chi^2 < 2$ for 4 additional parameters).

We find that the line is well resolved with a full width at half maximum (FWHM) velocity width of about $25,400 \text{ km s}^{-1}$, and a large equivalent width of about 275 eV (Table 2). The line width indicates that the X-ray emission is originating from a region close to the BH in Q0056-363. For a Keplerian disc, inclined at 30 degrees to the line of sight, this velocity implies that the iron line emission is occurring at a typical distance of 30 gravitational radii ($30R_g$) from the putative massive BH. The FWHM of the line is only about four times smaller than the one found in the Seyfert 1 MCG-6-30-15, which shows the most extreme broad FeK $_{\alpha}$ line observed up to now (e.g., $100,000 \text{ km s}^{-1}$, Tanaka et al. 1995; Wilms et al. 2001, Fabian et al. 2002, Lee et al. 2002). Since the line profile appears broad, and is likely to originate within

Table 2. Best-fitting spectral parameters in the 2.5–12 keV energy range for an absorbed ($N_{\text{H}}=1.88\times 10^{20} \text{ cm}^{-2}$) power-law (PL) component plus a line profile: GA: Gaussian profile; and DISKLINE and LAOR: profile line emitted by a relativistic accretion disk for a non-rotating BH and a maximally rotating BH, respectively (Fabian et al. 1989, Laor 1991). The line fluxes are expressed in $\text{erg cm}^{-2} \text{ s}^{-1}$. We assume an emissivity law q equal to -2. (a): $R_{\text{in}}=6 R_g$ and $R_{\text{out}}=1000 R_g$, inclination= 30° . (b): $R_{\text{in}}=1.26 R_g$ and $R_{\text{out}}=400 R_g$, inclination= 30° . (c): The energy of the line has been fixed to 6.4 keV (see text).

Model	Γ	Line parameters	$\chi^2/\text{d.o.f.}$
PL	1.98 ± 0.08		152.1/150
PL + GA	2.03 ± 0.09	$E=6.37_{-0.13}^{+0.18}$ keV $\sigma=0.23_{-0.11}^{+0.19}$ keV $F=9.6\pm 4.0\times 10^{-6}$ $EW=275_{-113}^{+164}$ eV	134.9/147
PL + DISKLINE ^(a,c)	2.03 ± 0.09	$F=8.4\pm 3.6\times 10^{-6}$ $EW=292\pm 124$ eV	137.2/149
PL + LAOR ^(b,c)	2.02 ± 0.09	$F=6.7\pm 3.6\times 10^{-6}$ $EW=229\pm 94$ eV	135.9/149

$30R_g$ of the BH, we proceed to fit the line with a profile expected from a relativistic accretion disk around a non-rotating (Schwarzschild) BH, using the DISKLINE model in XSPEC from Fabian et al. (1989). We find that such a profile, with a typical inclination of 30° for a type 1 AGN, emitted at a rest-frame energy of 6.4 keV, provides an excellent representation of the line observed in Q0056-363 (see Table 2). An equally good fit is obtained for a maximally rotating BH (Kerr) disc emission line model (LAOR; Laor 1991). A higher signal to noise ratio spectrum is required to discriminate between the Schwarzschild and the Kerr BH, and to determine the BH spin, if any.

The line profile and intensity are unusual for such a high X-ray luminosity AGN (i.e. $L_X > 10^{45} \text{ erg s}^{-1}$), where any broad line component is generally expected to be weak and highly ionised. As reported by Nandra et al. (1997), in a composite ASCA spectrum of high luminosity AGN, a very weak or negligible red wing is found in quasars whilst a blue (or ionised) side may be seen. Therefore the FeK $_{\alpha}$ line profile in Q0056-363 appears different from the average profile for such high luminosity objects, as the profile is consistent with a line emitted by a cold material in a relativistic accretion disk. The equivalent width of the line is also much stronger than that usually found in high luminosity quasars, where the overall strength of the line is thought to diminish with luminosity (e.g. Reeves & Turner 2000). The detection of broad iron lines appears to be rather rare for luminous quasars. We note that a weak, but broad iron line has been reported in the radio-loud quasar 3C 273 (Yaqoob & Serlemitsos 2000), from ASCA and RXTE observations. However any broad FeK $_{\alpha}$ line

profile present in a long (100 ksec) high signal to noise *XMM-Newton* observation of 3C 273 is very weak, at least down to the level of the systematic calibration uncertainties present in the PN detector, i.e. <5% of the continuum level at 6 keV (Reeves 2002). A broad iron line has recently been reported in the gravitationally micro-lensed quasar QSO 2237+0305 (Dai et al. 2003), from a *Chandra* ACIS observation. However it is likely that the (uncertain) intrinsic X-ray luminosity of this object is below 10^{45} erg cm $^{-2}$ s $^{-1}$. Broad ionised lines, possibly originating from a highly photoionised disc, have been observed in the high luminosity AGN, Mrk 205 and Mrk 509 (Reeves et al. 2001, Pounds et al. 2001), although both of these objects are a factor of 5-10 lower in X-ray luminosity than Q 0056-363. Q0056-363 is presently the highest luminosity *radio-quiet* quasar that exhibits such an intense and *broad* Fe K α line profile from low ionization iron.

4.2.1. Can X-ray disc reflection explain the Fe K α line?

Given the evidence for a broad iron line, where the emission is likely to originate from the inner accretion disc, we attempt to fit the X-ray spectrum of Q0056-363 with a disc reflection model. We use the ionised disc reflection model (XION) of Nayakshin et al. (2000), in the most simple configuration where the X-rays are emitted in a “lamppost” geometry at a height of $20R_g$ above the accretion disc. A ratio of X-ray to disc flux of 0.2 is assumed, appropriate for the lamppost geometry, as well as a high energy cut-off of 100 keV. This model provides an excellent fit above 2 keV ($\chi^2/d.o.f = 133.9/147$), matching the line profile of Q0056-363 very well. The best-fit of this lamppost ionised reflection model is extrapolated down to 0.3 keV and shown in Fig. 3. Whilst the model provides an excellent fit at high energies, the model fails to account for the strong soft X-ray excess observed below 2 keV, as there is not sufficient continuum curvature in the reflection model to account for the excess flux. Thus we can rule out disc reflection as the cause of the soft excess in Q0056-363. The derived parameters for the fit are: $\sim 25R_g$ for the inner disc radius (the outer radius is fixed at $1000R_g$), and $\sim 15^\circ$ for the disc inclination. We notice that the Fe abundance relative to Solar must be fixed to 5 in order to account for the high flux of the line. Interestingly a formal upper-limit is derived for the accretion rate of about 0.05 times the Eddington accretion rate. This low value of the accretion rate is being driven by the low value of the line energy (i.e. 6.4 keV) and the high equivalent width of the line. If one experiments with this model by increasing the accretion rate through the disc, then the line generally becomes more ionised (increasing to 6.7 keV), resulting in a worse fit. This is due to the formation of a highly ionised layer (dominated by He-like Fe) on the disc surface (e.g. Nayakshin & Kallman 2001) at higher accretion rates. We then relax the assumption that the X-ray emission originates in a simple lamppost geometry. A scenario whereby the emission arises through magnetic flares above the disc

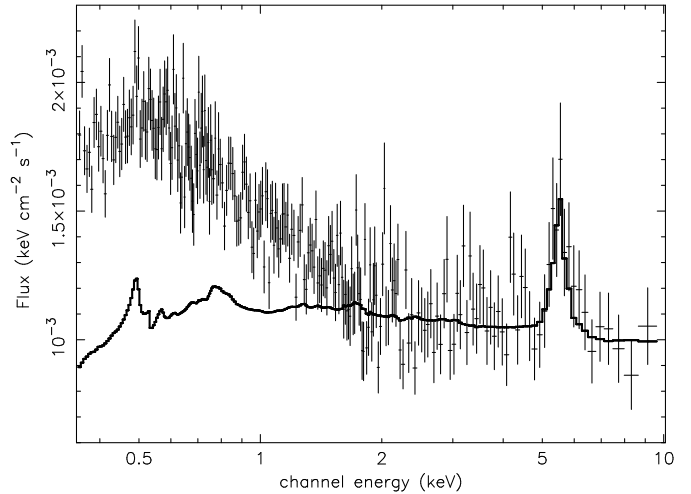


Fig. 3. Ionised disc reflection model fit to the PN spectrum of Q0056-363. This model (solid line) provides an excellent representation of the 2-12 keV spectrum and of the Fe K α line profile. However the reflection model does not explain the soft X-ray excess observed in Q0056-363 below 2 keV.

surface is adopted, the principle difference being that the X-ray emission occurs close to the surface of the disc (typically $1 R_g$), resulting in the ratio of local X-ray flux to disc flux being substantially higher. An equally good fit is obtained for the line profile ($\chi^2/d.o.f = 134.7/147$), with very similar parameters to those above. Again a low accretion rate (< 5% of Eddington accretion rate) is required to match the energy and strength of the line; increasing the accretion rate in the flare model leads to the formation of a deep, *fully ionised* layer of iron at the disc surface, weakening the iron line drastically.

The upper limit on the accretion rate (i.e. $\dot{m} < 5\%$) for the lamppost and the magnetic flare models is much lower than the value ($\sim 0.6-0.8$) inferred according to the spectral energy distribution of Q0056-363 (see sect. 3). This upper limit would be compatible with a much higher BH mass of about $7 \times 10^9 M_\odot$. Another possible alternative is a geometry whereby the X-ray source(s) is no longer point-like, but exists in a corona which covers most of the inner disc surface. In this scenario, the additional weight of the corona will increase the gas pressure and density at the surface layers of the disc, suppressing formation of a highly ionised layer, the result being that the gas remains cool and a line at 6.4 keV is observed (Nayakshin & Kallman 2001). The energy of the line in this case is largely independent of the accretion rate, presenting a plausible explanation of the iron line profile observed in Q0056-363. For a corona covering most of the disk, one would expect a large X-ray flux to UV flux ratio, but as is found in sect. 3, the luminosity in the *IUE* domain is about two times higher than in the *XMM-Newton* band. However a patchy corona, covering a large part (but not all) of the disc surface, could give a consistent explanation of the data.

A variability study of the line flux, and whether it is correlated or not with the continuum variability, is of

great interest and would provide a future test (in a longer observation) to discriminate between the above models. As discussed by Reynolds et al. (1999), the temporal response of the line contains important information on the accretion disk structure, the X-ray source geometry and on the BH spin. In the scenario of a dramatic flare in the disc corona, the intensity of the FeK $_{\alpha}$ line is expected to be constant even though the continuum flux varies significantly for outflowing magnetic flares with different bulk velocities (Lu & Yu 2001), while in the disc-corona geometry it is expected that the line responds rapidly to any change of the continuum.

Table 3. Best-fitting spectral parameters in the 0.3–12 keV energy range. COMPTT: Comptonization of soft photons in a hot plasma (Titarchuk 1994), and DISKLINE: profile line emitted by a relativistic accretion disk around a non-rotating BH (Fabian et al. 1989). (a): The soft photon temperature in the harder COMPTT component ($kT=100$ keV) has been fixed to the plasma temperature of the softer component. (b): $R_{\text{in}}=6 R_{\text{g}}$ and $R_{\text{out}}=1000 R_{\text{g}}$, inclination= 30° . (c): The line energy has been fixed at 6.4 keV in the quasar frame. (f): frozen parameter (see text).

2 COMPTT ^(a) + DISKLINE ^(b)	
kT _{photon1} =15 eV (f)	
kT _{plasma1} = 1.24 ^{+0.27} _{-0.22} keV	$\tau_1=6.6^{+0.5}_{-0.8}$
kT _{photon2} = kT _{plasma1} (tied)	
kT _{plasma2} = 100 keV (f)	$\tau_2=0.4^{+0.5}_{-0.3}$
F _{line} ^(c) =8.3±3.8×10 ⁻⁶ erg cm ⁻² s ⁻¹	EW=287±130 eV
F _{cont} ^{0.3–12 keV} =8.7 ^{+2.3} _{-2.0} ×10 ⁻¹² erg cm ⁻² s ⁻¹	
$\chi^2/\text{d.o.f.}=531.3/524$	

4.3. Can Comptonization explain the broad soft X-ray excess in Q0056-363?

Comptonization has often been suggested as a source of both the soft X-ray and hard X-ray spectra of AGN. For example the accretion disk may be responsible for the EUV/soft X-ray emission, with some of these soft photons being inversed-Compton scattered into the hard X-ray energy range, as they pass through the hot corona above the disc. We further investigate such models over the 0.3-12 keV range, by using the COMPTT model in XSPEC (Titarchuk 1994). We first test a model with one absorbed COMPTT component, using single electron temperature, plus a DISKLINE profile; we obtain an unsatisfactory fit with $\chi^2/\text{d.o.f.}=664/524$, as this model failed to account for all of the soft excess present in the X-ray spectrum. Instead we test a double Comptonization model, in this model we assume that there are two layers of Comptonising electrons, whereby the output from the first cooler one is in turn Comptonized by the hotter

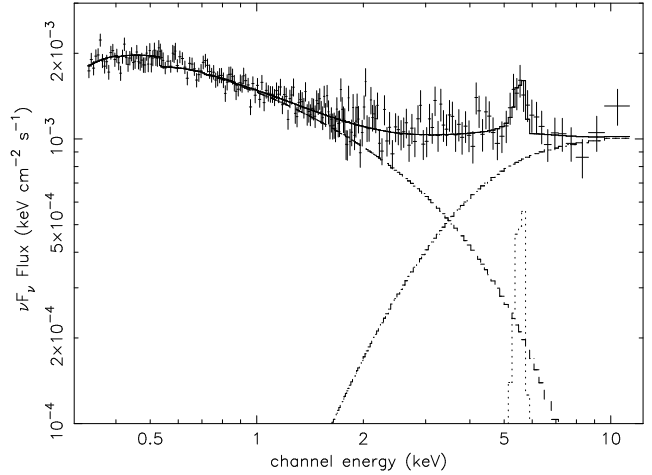


Fig. 4. The unfolded νF_{ν} PN spectrum (0.3–12 keV) fitted with a double Comptonization model (COMPTT, Titarchuk 1994) and a line profile from a relativistic accretion disk (DISKLINE, Fabian et al. 1989).

component (i.e. $kT_{\text{photon2}}=kT_{\text{plasma1}}$). We fix the input soft photons temperature (kT_{photon1}) of the first COMPTT component to 15 eV (see sect. 4.1 for explanation). Since our spectral bandpass (up to 12 keV) does not enable us to constrain the cut-off energy for the hard power-law, the temperature of the hotter Comptonization component (kT_{plasma2}) has been fixed at 100 keV. The inferred parameters are reported in Table 3, a very good fit is obtained, the model manages to reproduce all of the spectral curvature seen in the *XMM-Newton* spectrum of Q0056-363. The largest part of the flux, i.e. about 67%, is emitted in the 0.3–2 keV energy band. As an illustration, Fig. 4 shows the corresponding 0.3–12 keV unfolded PN spectrum (in νF_{ν} units). In this model, a hot (or even non-thermal) electron plasma is responsible for the power-law like emission above 2 keV, whilst a lower temperature component is responsible for the soft excess below 2 keV. One possibility is that the cooler Comptonizing component arises from a hot disc skin or atmosphere whilst the hotter one originates from the corona (e.g. produced through magnetic reconnection). Alternatively there may be only one Comptonizing layer with a non-thermal distribution of electrons (i.e. responsible for the hard X-ray power-law), the low energy portion of which becomes Maxwellian (i.e. thermalised) and produces the soft excess (e.g. see Vaughan et al. 2002 for a discussion on the soft X-ray excess in the narrow-line Seyfert 1 Ton S180).

While the broad-band X-ray continuum of Q 0056-363 can be explained by a double comptonization model, this model does not directly account for the emission line at 6.4 keV or the reflected continuum from the disc. Therefore we attempted to combine the thermal Comptonization model with the X-ray disc reflection model XION from Nayakshin et al. (2000), which can account for the line at 6.4 keV. The model XION can only be directly linked to a power-law continuum model, therefore we fit the data with a combination of the COMPTT model (at soft X-ray energies)

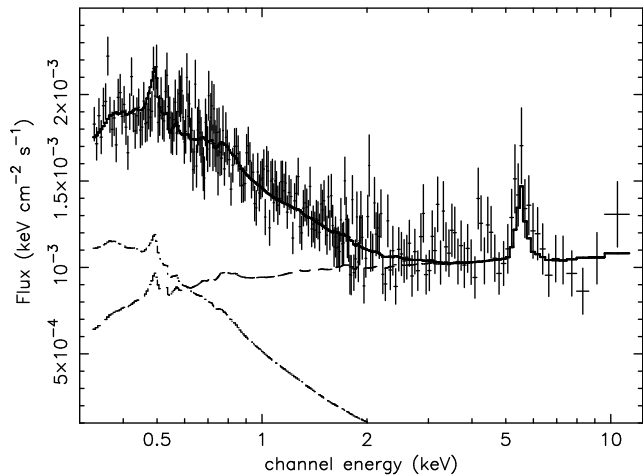


Fig. 5. The unfolded νF_ν PN spectrum (0.3–12 keV) fitted with a combination of the COMPTT model (at soft X-ray energies) and a power-law continuum model which mimics the hard Comptonization component, with an X-ray disc reflection model (XION).

and a power-law continuum model which mimics the hard Comptonization component, with an X-ray disc reflection model (XION). As the previous fits, we fix the disc photon temperature to 15 eV, and we assume for simplicity a lamppost geometry. We fix the relative abundance of the iron to 5. We find a very good representation of both the line at 6.4 keV and the underlying continuum from 0.3 to 12 keV ($\chi^2/\text{d.o.f.}=533.1/522$), with $kT=0.34_{-0.07}^{+0.10}$ keV and $\tau=12.5_{-2.0}^{+2.3}$ (for the cool comptonized layer), $\Gamma=1.98_{-0.08}^{+0.07}$ (hot comptonized layer), $\dot{m} < 13\%$, a disc inclination of less than 31° , and an inner accretion disc radius of $48_{-23}^{+73} R_g$. We find an unabsorbed 0.3–10 keV flux of $8.4 \times 10^{-12} \text{ erg cm}^{-2} \text{ s}^{-1}$ and a corresponding 0.3–10 keV luminosity of $1.2 \times 10^{45} \text{ erg s}^{-1}$, with about 67% is emitted below 2 keV. The unfolded 0.3–12 keV unfolded PN spectrum (in νF_ν units) is plotted in Fig. 5.

5. Conclusion

We find that Q0056-363 is a powerful quasar in the X-ray band, with a 0.3–12 keV unabsorbed luminosity of about $1.2 \times 10^{45} \text{ erg s}^{-1}$ with the largest part ($\sim 67\%$) emitted below 2 keV. The 0.3–12 keV broad band X-ray spectrum of Q0056-363 is dominated by a strong soft X-ray excess, and displays a broad and intense FeK α line at 6.4 keV. Q0056-363 is presently the most luminous AGN known to exhibit such a broad and intense FeK α line profile from near neutral iron. The 0.3–12 keV broad band spectrum of Q0056-363 may be represented by the combination of Comptonization and X-ray disc reflection: the cool layer of comptonizing electrons ($kT=0.3\text{--}1.2$ keV) is then comptonized by the hot layer ($kT=100$ keV), and the output of that illuminates the disk which emits the line at 6.4 keV. A high relative abundance of the iron of about 5 is required to account for the intensity of the line for the disc

reflection models. A rather low value for the quasar accretion rate (of $<5\text{--}13\%$ of the Eddington rate) is inferred from disc reflection models and is not compatible with the rate inferred from the spectral energy distribution of Q0056-363, unless the black hole mass is much higher than the value found according to the relation between H_β line widths and flux. One alternative is that the source of X-rays is a patchy corona covering a large part of the inner disc surface.

Future high signal to noise observations by *XMM-Newton* of Q0056-363 will help to discriminate between a non rotating BH or a rotating BH and to determine the BH spin if any. In addition to this, observations of other bright, high luminosity quasars, will help to determine whether the FeK α line in Q0056-363 is truly unusual or not. Studying the properties of the FeK α line in a variety of AGN, spanning a wide range of physical parameters (black hole mass and spin, accretion rate, radio-loudness) can provide a potentially powerful diagnostic of the accretion process and of the geometry of the X-ray emission.

Acknowledgments

Based on observations obtained with the XMM-Newton, and ESA science mission with instruments and contributions directly funded by ESA member states and the USA (NASA). We thank the anonymous referee for very fruitful comments and suggestions. D.P. acknowledges N. Grosso for his help for the management of the multi-wavelength archived observations of Q0056-363. D.P. acknowledges grant support from MPE fellowship.

References

- Anders, E. & Grevesse, N., 1989, *Geochimica et Cosmochimica Acta*, 53, 197
- Arnaud, K.A., Branduardi-Raymont, G., Culhane, J.L., et al., 1985, *MNRAS*, 217, 105
- Campins, H., Rieke, G.H., Lebofsky, M.J. 1985, *AJ*, 90, 896
- Cutri, R.M., Skrutskie, M.F., Van Dyk, S. et al. 2003, <http://www.ipac.caltech.edu/2mass/releases/allsky/index.html>
- Dai, X., Chartas, G., Agol, E., Bautz, M.W., Garmire, G., 2003, *ApJ*, 589, 100
- den Herder, J.W. et al., 2001, *A&A*, 365, L7
- Fabian, A.C., Rees, M.J., Stella, L., White, N.E. 1989, *MNRAS*, 238, 729
- Fabian, A.C., Vaughan, S., Nandra, K. et al., 2002, *MNRAS*, 335, L1
- Grupe, D., Beuermann, K., Mannheim, K., Thomas, H.-C., 1999, *A&A*, 350, 805
- Grupe, D., Thomas, H.-C., Beuermann, K., 2001, *A&A*, 367, 470
- Hewitt, A. & Burbidge, G. 1989, *ApJS*, 69, 1
- Laor, A., 1991, *ApJ*, 376, 90
- Lee, J.C., Iwasawa, K., Houck, J.C., Fabian, A.C., Marshall, H.L., Canizares, C.R. 2002, *ApJ*, 570, L47
- Lu, Y. & Yu, Q. 2001, *ApJ*, 561, 660
- McLure, R.J. & Dunlop, J.S. 2002, *MNRAS*, 331, 795
- McLure, R.J. & Jarvis, M. J. 2002, *MNRAS*, 337, 109

- Monet, D.G., Levine, S.E.; Canzian, B. et al. 2003, AJ, 125, 984
- Monk, A.S., Penston, M.V., Pettini, M., Blades, J.C., 1986, MNRAS, 222, 787
- Nandra, K., George, I.M., Mushotzky, R.F., Turner, T.J., Yaqoob, T., 1997, ApJ, 488, L91
- Nayakshin, S., Kazanas, D., Kallman, T., 2000, ApJ, 537, 833
- Nayakshin, S. & Kallman, T., 2001, ApJ, 546, 406
- O'Donnell, J.E. 1994, ApJ, 422, 158
- Peterson, B.M. 1997, An introduction to active galactic nuclei, New York Cambridge University Press.
- Porquet, D., Dumont, A.-M., Collin, S., Mouchet, M., 1999, A&A, 341, 58
- Pounds, K., Reeves, J., O'Brien, P., Page, K., Turner, M., Nayakshin, S., 2001, ApJ, 559, 181
- Pounds, K. & Reeves, J. 2002, 'New Visions of the X-ray Universe in the XMM-Newton and Chandra Era', in press [astro-ph/0201436]
- Reeves, J.N. & Turner, M.J.L., 2000, MNRAS, 316, 234
- Reeves, J.N., Turner, M.J.L., Pounds, K.A., O'Brien, P.T., Boller, T., Ferrando, P., Kendziorra, E., Vercellone, S., 2001, A&A, 365, L134
- Reeves, J.N. 2002, to appear in proceedings of: "Active Galactic Nuclei: from Central Engine to Host Galaxy", ASP Conference Series, in press [astro-ph/0211381]
- Reynolds, C.S. & Fabian, A.C., 1995, MNRAS, 273, 1167
- Reynolds, C.S., Young, A.J., Begelman, M.C., Fabian, A.C. 1999, ApJ, 514, 164
- Ryter, C.E. 1996, Astrophysics and Space Science, 236, 285
- Schlegel, D.J., Finkbeiner, D.P., Davis, M. 1998, ApJ, 500, 525
- Seaton, M.J. 1979, MNRAS, 187, 73P
- Strueder, L., et al., 2001, A&A, 365, L5
- Tanaka, Y., Nandra, K., Fabian, A.C., et al., 1995, Nature, 375, 659
- Thomas, H.-C., Beuermann, K., Reinsch, K., Schwope, A.D., Trümper, J., Voges, W., 1998, A&A, 335, 467
- Titarchuk, L., 1994, ApJ, 434, 570
- Turner, T.J. & Pounds, K.A., 1989, MNRAS, 240, 833
- Turner, M.J., Abbey, A., Arnaud, M. et al., 2001, A&A, 365, L27
- Vaughan, S., Boller, T., Fabian, A.C., Ballantyne, D.R., Brandt, W.N., Trümper, J. 2002, MNRAS, 337, 247
- Wilms, J., Allen, A., McCray, R., 2000, ApJ, 542, 914
- Wilms, J., Reynolds, C.S., Begelman, M., et al., 2001, MNRAS, 328, L27
- Yaqoob, T. & Serlemitsos, P. 2000, ApJ, 544, L95